Strategy for Active Power Sharing in a Fuel-Cell-Powered Charging Station for Advanced Technology Batteries

Zhenhua Jiang and Roger A. Dougal
Department of Electrical Engineering
University of South Carolina
Columbia, SC 29208

Abstract– This paper presents a novel real-time strategy for active power sharing in a fuel-cell-powered charging station for advanced technology batteries. This control scheme can adjust the charging currents according to the estimated state-of-charge which is obtained by estimating the battery open-circuit voltage with current correction and linearly fitting between the open-circuit voltage and the state-of-charge. Both DC and pulse current charging strategies are investigated to coordinate the active power distribution among batteries. The DC charging controller is designed and implemented in MATLAB/Simulink for both system simulation and experimental tests. Simulation and experimental results are also given.

I. INTRODUCTION

The limited usable time of rechargeable batteries, which are playing an increasingly significant role in the utilization of portable electronic devices such as portable computers, cellular phones and camcorders [1], makes it essential to develop some kind of portable battery charging system. The fuel cell, which is emerging as one of the most promising technologies for the future power sources [2-3], may provide a good solution for powering the portable charging station [4-5], which may be far away from the utility power. However, when charging advanced technology batteries such as Li-Ion cells, it is hazardous to exceed certain current or voltage limits. The fuel cell has a limited power capacity, and large power demand may go beyond its power limit. Both the fuel cell and lithium ion battery are strongly nonlinear [6-9]. All of these present a lot of difficulties for the control design.

In order to meet the simultaneous requirements of multiple users, power converters are connected in parallel, each for one battery pack. In the general case, the initial states of the batteries being inserted are considerably different. A battery with lower initial state-of-charge (SOC) may require a larger charging current or otherwise a longer charging time. Therefore, the power from the fuel cell should be distributed efficiently among the charging branches. Three basic static control schemes have been investigated in [5]. Under equal rate charging strategy, the battery with the highest initial state-of-charge can become full fastest but the total charging time is the longest. Proportional rate charging strategy and pulse current charging strategy change the situation and it is possible for all the batteries to become fully charged almost simultaneously. However, with these static strategies, the charging currents or the duty cycles of the pulse currents are set up at the very beginning according to the estimation of the initial states and do not change any more during the current regulation mode. The simultaneous termination of charging is not guaranteed. In order to reduce the total charging time and the fuel use, the current sharing among battery banks should be optimized in real time and vary with the state-of-charge of each battery.

The state-of-charge is a defined variable that is used to represent the charge remaining in the battery and it is widely used in the electrochemical field. However, it can not be measured directly and it also is difficult to estimate the state-of-charge. Many people have studied the approaches to the state-of-charge estimation. Liu presented two methods in [10] to estimate the state-of-charge, whereas the ampere-hours method requires the information of initial state-of-charge and the recursive method needs a lot of offline experimental data to obtain the many parameters. In this application, a simple and practical approach may be desired to estimate the state-of-charge based on the measured charging current and voltage of the battery.

This paper presents a novel real-time control strategy (RTCS) for active power sharing in a fuel-cell-powered battery-charging station. This control strategy can adjust the charging currents according to the estimated state-of-charge which is obtained by estimating the battery open-circuit voltage with current correction and linearly fitting between the open-circuit voltage and state-of-charge. Both DC and pulse current charging strategies are investigated to coordinate the active power distribution among batteries. The DC charging controller is designed and implemented in MATLAB/Simulink for both system simulation and experimental tests. Simulation and experimental results are also given.

II. SYSTEM DESIGN AND PROBLEM DEFINITION

In general, the battery charging station should allow multiple batteries to be charged simultaneously, and it should be possible to insert or retrieve any battery at any time. A typical case of three charging channels is studied in this paper, which can represent the general solution of many charging channels. Assume here that all of the three batteries are in the charger. The case that some batteries are inserted or retrieved during charging is studied in [11].

0-7803-7754-0/03/$17.00 ©2003 IEEE

The block diagram of the fuel-cell-powered battery-charging station is shown in Figure 1, where the parameters are also shown. A fuel cell stack, which is the power generation system, is used to charge up to three lithium ion battery packs, each through a buck converter. Each battery contains four series-connected cells. The buck converters condition the power to the batteries. By controlling the buck converters, the charging currents and battery voltages can be regulated. A digital controller is used to coordinate the power converters. The real-time control strategy for active power sharing in this fuel cell/battery system is implemented in this controller. The charging currents and battery voltages are monitored and fed to the controller. This digital controller can calculate the reference charging current for each channel and the corresponding duty cycle. It can also output the PWM switching waves to the drivers of the switches in buck converters.

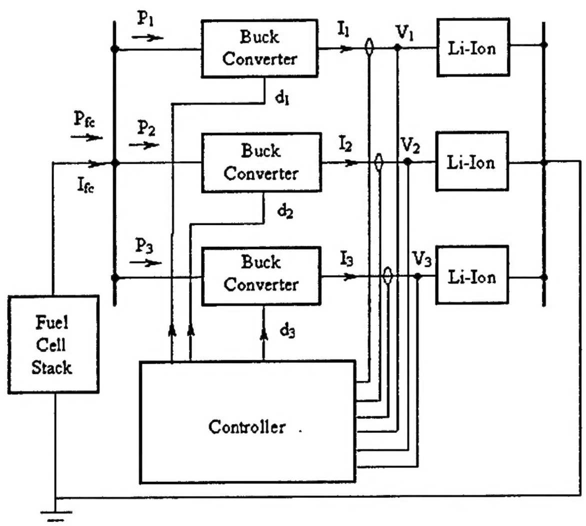

Figure 1. Block diagram and parameter definition of the fuel-cell-powered battery-charging station.

From Figure 1, it is shown that the active power from the fuel cell is distributed among the three batteries, which can be expressed in (1).

$$P_{fc} = P_1 + P_2 + P_3 \tag{1}$$

where P_1, P_2, and P_3 are the power to three charging channels respectively, and P_{fc} is the power from the fuel cell.

In practice, the power distribution among the batteries is realized by regulating the charging currents of the batteries. The following equation relates the current from the fuel cell to three charging currents.

$$I_{fc} = d_1 I_1 + d_2 I_2 + d_3 I_3 \tag{2}$$

where I_1, I_2, and I_3 are the average current to three batteries respectively, I_{fc} is the current of the fuel cell, and d_1, d_2, d_3 are the duty cycles of three buck converters respectively and have values between 0 and 1.

Since the fuel cell current is limited, the sum of the right hand side in (2) should be less than some value. Considering that the variations in the voltages of the fuel cell and batteries are not too large, the duty cycle will vary within a limited small range, for example, between 0.7 and 0.75. Based on this assumption, we can take the following expression as a criterion for power distribution among the batteries.

$$I_1 + I_2 + I_3 \le I_{\text{lim}} \tag{3}$$

where I_{lim} is a preset limit for the total charging current.

Equation (3) gives a basic requirement for design of active power sharing strategy. Actually, the goal of the real-time control strategy is to utilize the power of the fuel cells efficiently and to distribute the power among batteries reasonably.

III. Strategy for Active Power Sharing

A. Real-Time Control Strategy

The users may have different requirements for charging their batteries according to their own needs. Some people may require that the batteries be fully charged within the shortest period of time, while others may need a better life expectation for their batteries. This paper, aiming to discover an appropriate control scheme for minimizing the charging time, investigates a real-time control strategy for DC and pulse current charging to coordinate the active power sharing. DC charging protocol can help to protect the battery from overcharging. Under this protocol, the battery is charged to an end potential using a DC current. The potential is then held constant after this potential is reached, and the charging current will taper gradually. Charging stops when the current reaches a preset small value during the constant voltage mode. Pulse current charging has been shown to enhance charging rate capability and also prevent the increase of internal impedance of the battery, thus reducing the total charging time [9]. Under pulse charging protocol, a pulse current with a period of *T* and on-time of *Ton* is applied to the battery.

In order to discover the real-time control strategy, let's consider a basic relationship between the battery capacity and charging current. The capacity of the battery can be expressed as follows.

$$C(t_{end}) = C_0 \cdot SOC_0 + \int_0^{t_{end}} I \cdot dt \tag{4}$$

where C_0 is the rated capacity of the battery, SOC_0 is the initial state-of-charge, I is the charging current, t_{end} is the total time for charging. From (4), it is seen that the charge that the battery will need to get fully charged is the integral of the

charging current over the total charging time. The depth of discharge can be used to represent a measurement of the rest of charge. It is calculated as unity minus state-of-charge. If direct currents of the same magnitude are applied to charge different batteries, the charging time will be proportional to the depth of discharge (neglecting nonlinearity). On the other hand, if we want all the batteries to become fully charged at the same time, the charging current can be proportional to the fraction of the depth of discharge of each battery. Therefore, the charging current for each battery can be calculated according to (5)

$$I_i = I_{\lim} \cdot \frac{1-SOC_i}{\sum_{i=1}^{3}(1-SOC_i)}, i=1,2,3 \tag{5}$$

where I_i is the charging current of the *ith* battery, I_{lim} is the total available charging current, and SOC_i is the initial state-of-charge of the *ith* battery. It is clear that the current sharing strategy shown in (5) meets the criterion given in (3) and utilizes as much power of the fuel cell as possible.

For pulse current charging, three pulse currents with the same period of T and different pulse-durations are applied to three batteries alternatively. The sum of the pulse-duration of each current is equal to the period. The illustration of this control strategy is given in Figure 2. A similar strategy as DC charging can be found for pulse charging. The duty cycles of pulse charging currents can be proportional to the fraction of the depth of discharge of each battery, which can be estimated according to the following equation.

$$D_i = \frac{1-SOC_i}{\sum_{i=1}^{3}(1-SOC_i)}, i=1,2,3 \tag{6}$$

where D_i is the duty cycle of the charging current of the *ith* battery. Under this strategy, the charging current can be relatively large because only one battery draws this current at any time.

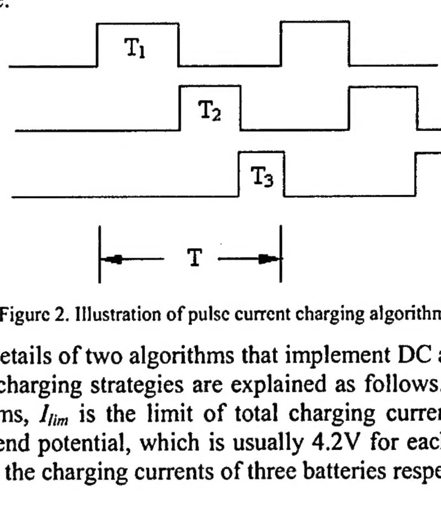

Figure 2. Illustration of pulse current charging algorithm.

The details of two algorithms that implement DC and pulse current charging strategies are explained as follows. In these algorithms, I_{lim} is the limit of total charging current. V_{ref} is battery end potential, which is usually 4.2V for each cell. I_1, I_2, I_3 are the charging currents of three batteries respectively.

A. Algorithm 1: DC charging

- $I_{ref,i}=I_{lim}*(1-SOC_i)/[(1-SOC_1)+(1-SOC_2)+(1-SOC_3)]$, $i=1, 2, 3$
- If $V_1= V_{ref}$, I_1 is tapering
- If $V_2= V_{ref}$, I_2 is tapering
- If $V_3= V_{ref}$, I_3 is tapering
- If $I_i<0.1 \times I_{ref,i}$, then $I_{ref,i}=0$, where $i=1,2,3$

B. Algorithm 2: Pulse current charging

- $I_{high,ref}=I_{lim}$, and $I_{low,ref}= I_{lim} \times 1\%$
- $D_{ref,i}=(1-SOC_i)/[(1-SOC_1)+(1-SOC_2)+(1- SOC_3)]$
- If $V_{low,i}>= V_{ref}$, then $I_{ref,i}=0$, $i=1,2,3$

B. Battery State-of-Charge Estimation

In the above algorithms, the charging currents and duty cycles of pulse currents vary with the state-of-charge. Since it is impossible to measure the state-of-charge directly, a method should be found to estimate the state-of-charge according to the measured battery voltage and charging current. For Li-Ion batteries, an approximate relationship between the state-of-charge and open-circuit voltage can be found when the state-of-charge is not within the extreme range, i.e., if the state-of-charge is between 0.1 and 0.9. Therefore, the state-of-charge can be estimated by measuring the battery voltage. In this paper, the state-of-charge is estimated according to a linear relationship, which is given in (7).

$$SOC = \begin{cases} 0.9, & v_0 > v_1 \\ \dfrac{v_0 - a}{b} + c, & v_2 < v_0 < v_1 \\ 0.1, & v_0 < v_2 \end{cases} \tag{7}$$

where a, b and c are constants and can be easily obtained through a series of experiments, v_0 is the battery open-circuit voltage. This estimation is shown in Figure 3. When the state-of-charge is greater than 0.9, the battery charger is usually working under constant voltage mode and the battery voltage does not change. The charging current is not determined by the charge controller itself, but by the internal potential and terminal voltage of the battery. It is not necessary to estimate the state-of-charge since the information about state-of-charge is useful only when the charger works under current regulation mode. When the state-of-charge is less than 0.1, the estimation is cut off to 0.1. In this case, the estimated value for depth of discharge is 0.9, and the fraction of the depth of discharge is very close to that using a more accurate value of the state-of-charge. This approximation does not affect the performance of the charging algorithm significantly, as will be shown later in simulation and experiment.

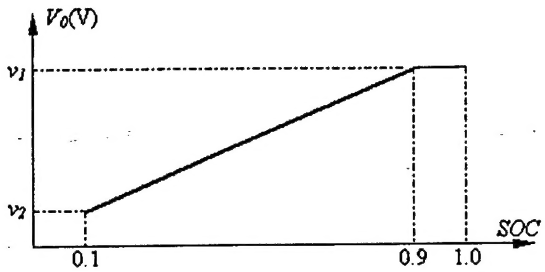

Figure 3. Linear fitting between the open-circuit voltage and the state-of-charge of the battery.

When the battery is being charged, it is impossible to measure the open-circuit voltage directly. But when the battery is open, the terminal voltage is equal to the internal potential of the battery, which does not change when an external voltage is imposed across it at this time. A simplified equivalent circuit of the battery when an external charging voltage is applied to the battery is illustrated in Figure 4.

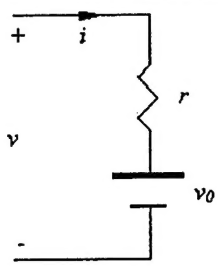

Figure 4. Illustration of the equivalent circuit for estimation of the open-circuit voltage of the battery.

From Figure 4, it is clear that the battery open-circuit voltage can be estimated from the following equation.

$$v_0 = v - i \cdot r \tag{8}$$

where v and i are the measured battery voltage and charging current respectively, r is the equivalent series resistance (ESR) of the battery.

The proposed method for state-of-charge estimation is very simple and easily realized. Essentially, we need only to estimate the state-of-charge in order to decide how to divide the available current between the batteries. The actual state-of-charge is not of interest to this current distribution strategy, although it is useful in determining when the charging process terminates. If the estimate differs from actual state-of-charge, it only means that it takes slightly longer to charge the system of batteries because some battery gets less than its fair share of the current.

IV. Implementation of Charge Controller

Mathworks' MATLAB/Simulink was selected as the tool for the control system design for two reasons. First, an interface to Matlab/Simulink is available in the VTB environment which makes it possible to test the control algorithm with very detailed models of all of the hardware components, including fuel cell, batteries, and power electronics. Secondly, the Matlab software provides an interface layer to dSpace hardware. The experimental validation can be performed by compiling Simulink codes of the controller and downloading onto the DSpace platform to control the real hardware.

Implementation of pulse current charging algorithm is similar to that of DC charging algorithm. In the following, we take DC charging algorithm as an example. The Simulink model of the controller for DC charging is shown in Figure 5. The main functional blocks in the controller are the charging current strategy module, current regulation module, voltage regulation module, and charging termination decision module.

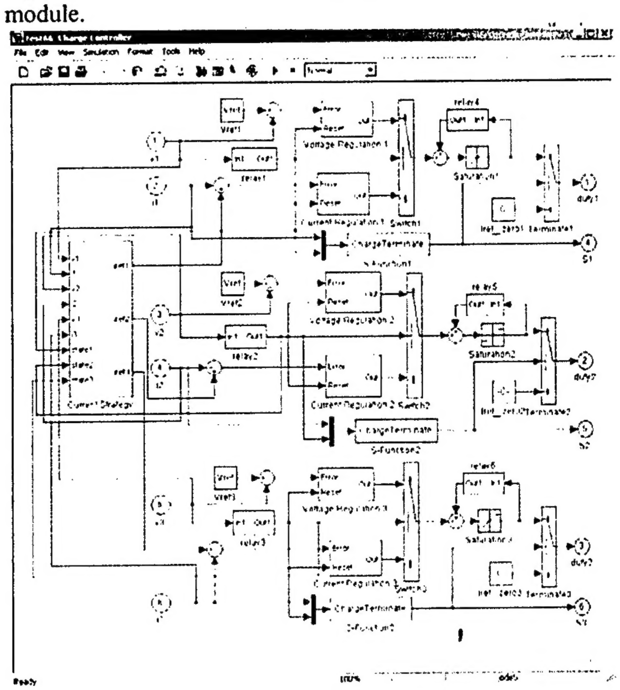

Figure 5. Simulink model of the proposed battery charge controller for DC charging.

The charging current strategy module is to calculate the reference charging currents according to the measured battery voltages and currents and it is developed based on the proposed DC current sharing algorithm which is shown in (5), (7) and (8). The Simulink model for this module is shown in Figure 6. The total available charging current is calculated according to the regulation mode and the charging currents. The depth of discharge is estimated for each battery based on the measured voltage and current. Based on these, the reference charging current for each channel is obtained.

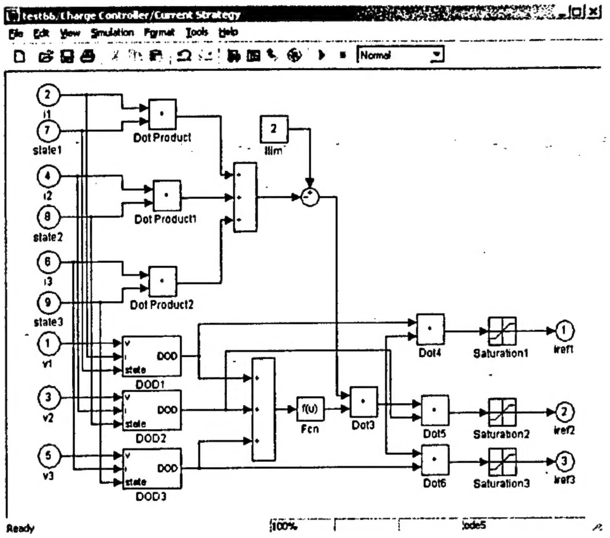

Figure 6. Model for charging current strategy module.

The current and voltage regulation modules are used to compute the duty cycles to the buck converters according to the reference currents from the charging current strategy module and the reference voltages respectively. The classical proportional-integral approach is used to regulate the charging currents and voltages. The current and voltage regulations are formulated in (9) and (10) respectively.

$$d = d_{old} + k_{pi}(I_{ref} - I) + k_{ii}\int(I_{ref} - I)dt \qquad (9)$$

$$d = d_{old} + k_{pv}(V_{ref} - V) + k_{iv}\int(V_{ref} - V)dt \qquad (10)$$

where V, I are the sampled voltage and current of the battery, d and d_{old} are the current and previous duty cycles used to control the buck converter, V_{ref} and I_{ref} are the reference voltage and charging current of the battery, k_{pi}, k_{ii}, and k_{pv}, k_{iv} are proportional and integral gains for current and voltage respectively.

The charging termination decision module can determine when the charging stops and output a signal to the corresponding power converter.

V. Simulation Results

In order to investigate the performance of the proposed real-time control strategy, a simulation study was first conducted in the VTB [12], which is endowed with mechanisms for importing models from MATLAB and co-simulating with Simulink. The system shown in Figure 1 was simulated in VTB for 2 hours (7200 seconds). The VTB schematic view of this system is shown in Figure 7. The initial states-of-charge of the batteries are 0.45, 0.50, and 0.55 respectively. The total available charging current is 2 Amperes.

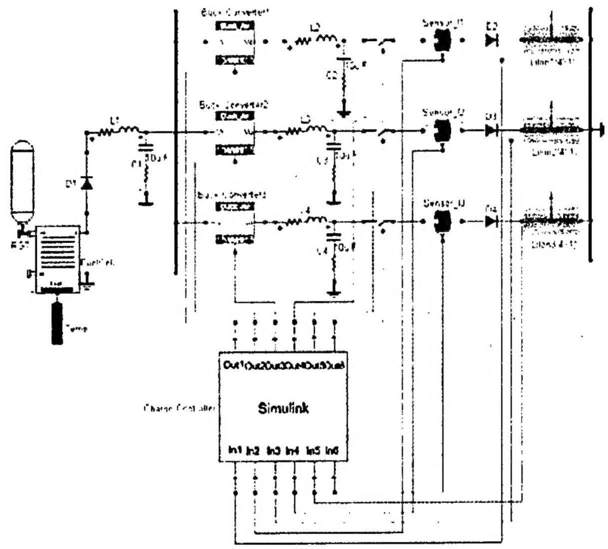

Figure 7.VTB schematic view of the fuel-cell-powered battery-charging station.

The controller is implemented in the Simulink model as shown in Figure 5 and embedded to VTB simulation. The simulated charging currents and states of charge of the batteries under the proposed real-time control strategy are shown in Figure 8. From the simulation results, it is seen that the battery with the highest state-of-charge is charged at the lowest current. The charging currents vary with the estimated state-of-charge. Under this real-time control strategy, all the batteries get the same state-of-charge at the end of charging.

In the simulation, the control algorithm was tested on a highly accurate non-linear model of the battery. Even though a really simple state-of-charge estimate is made from the linear model, simulation results show the difference between the rough estimate and the exact state-of-charge does not significantly impact the system performance.

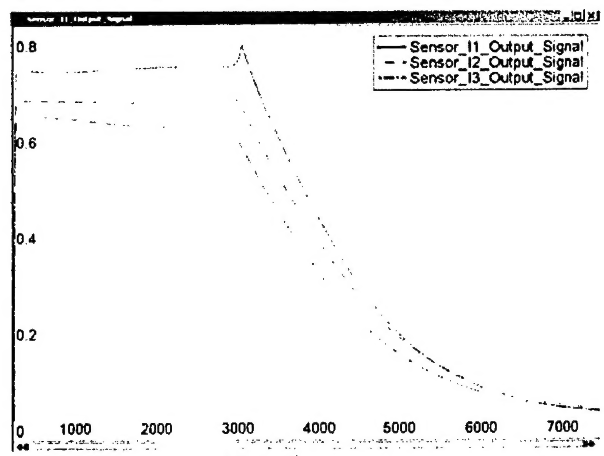

(a) charging currents

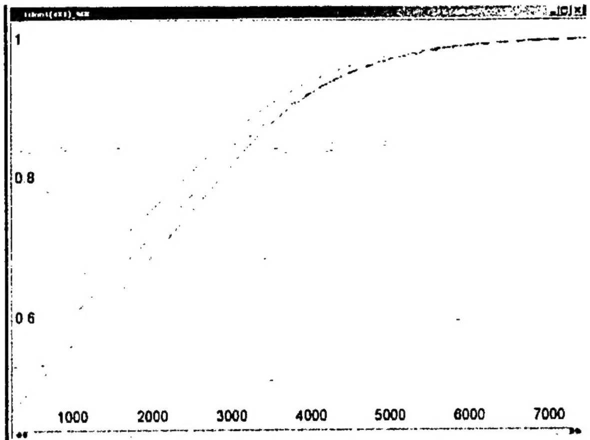

(b) states of charge

Figure 8. Simulation results for the charging currents and states of charge of three batteries.

VI. EXPERIMENTAL RESULTS

After simulation results showed that the real-time control strategy provided good coordination for the active power distribution, it was next validated with real hardware. A prototype of the fuel cell powered battery charging station was built using an H-Power D35 PEM fuel cell stack as the power source. This stack has a nominal power capacity of 35W and nominal 24V open circuit voltage. Three 4-cell Panasonic lithium ion batteries were used. The nominal capacity of each battery is 1500mAh. Three buck converters were built on one single board to distribute the charging current. The block diagram of the experiment environment is shown in Figure 9. The charging algorithm implementing the real-time control strategy resides on a general-purpose dSPACE real-time controller board, which also houses the hardware interface consisting of multi-channel A/D and D/A converters. The charging control algorithms are designed and implemented using MATLAB/ Simulink and the codes are then compiled and dropped onto a dSPACE DS1103 PPC controller board to control the real hardware. The charging currents and battery voltages are monitored and input to the dSPACE controller board through the A/D converters mounted on it. The power source bus voltage is also an input variable for monitoring purpose. The real-time controller provides the switch duty commands to each buck converter. The circuit protection function is also implemented within the software.

The experimental testing was conducted with DC charging algorithm. In order to ensure that each charging current would never exceed the safe maximum charging current (that is 800mA for the batteries used in the experiment), the total charging current was scaled down to 1 Ampere. The initial open-circuit voltages of the batteries were 16.3V, 16.4V, and 16.2V respectively. Figure 10 shows the measured voltages and charging currents of three batteries.

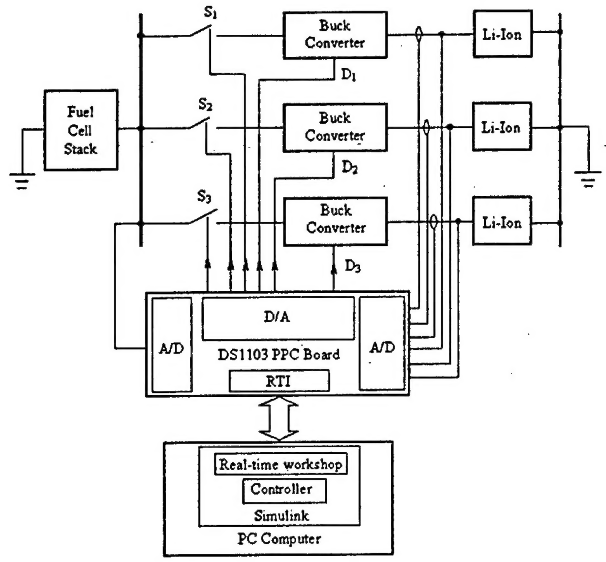

Figure 9 Block diagram for the experiment setup.

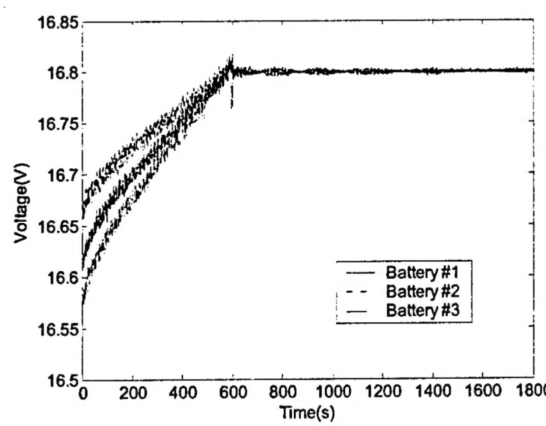

(a) From top to down: voltages of batteries #2, #1, and #3

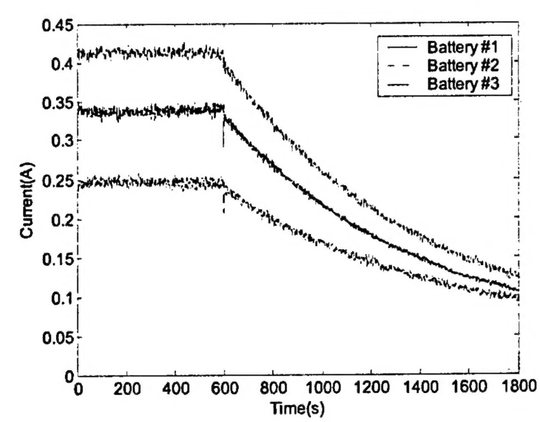

(b) From top to down: voltages of batteries #3, #1, and #2

Figure 10. The measured battery voltages and charging currents: (a) voltages, (b) currents.

From Figure 10, it is shown that during current regulation mode the battery voltages were different and the charging currents varied with the voltage in real time. The battery with the lowest initial voltage (and thus the least initial charge) was charged with the highest current, and its voltage increased more rapidly than the others. This was also predicted by the simulation. From the experimental results, it is also seen that the proposed method for battery state-of-charge estimation was effective for the active power sharing strategy.

VII. CONCLUSION

This paper presents a novel real-time control strategy for active power sharing in a fuel-cell-powered battery-charging station. DC charging algorithm is developed to regulate the power distribution among batteries. The charging controller is designed and implemented in MATLAB/Simulink for both system simulation and experimental tests. Simulation and experimental results show that the proposed control strategy for active power sharing can change the charging currents according to the estimation of state-of-charge in real time. The proposed method for battery state-of-charge estimation is effective for the active power sharing strategy. It is also seen that the batteries can become fully charged almost simultaneously under the proposed algorithm.

ACKNOWLEDGEMENTS

This work was supported in part by the US CECOM and the NRO under contract NRO 000-01-C-4368, and by US ONR under contract N00014-00-1-0368 and under contract N00014-00-1-0131.

REFERENCES

[1] R. J .Brodd, "Overview: rechargeable battery systems", *Conf. Record of WESCON'93*, pp. 206 –209, 1993.

[2] B. Rohland, J. Nitsch, and H. Wendt, "Hydrogen and fuel cells-the clean energy system", *Journal of Power Sources*, Vol. 37, No. 1-2, pp. 271-277, January 1992.

[3] A. Heinzel, C. Hebling, M. Müller, M. Zedda and C. Müller, "Fuel cells for low power applications", *Journal of Power Sources*, Vol. 105, No. 2, pp. 148-153, March 2002.

[4] Z. Jiang and R. Dougal, "Design and testing of a fuel-cell-powered battery-charging station", *Journal of Power Sources*, Vol. 115, No. 2, pp. 148-153, April 2003.

[5] Z. Jiang and R. Dougal, "Control design and testing of a novel fuel-cell-powered battery-charging station", *Proceedings of IEEE Applied Power Electronics Conference*, Miami, FL, pp. 1127-1133, Feb. 9-13, 2003.

[6] M. M. Bernardi, and M. W. Verbrugge, "A mathematical model of the solid-polymer-electrolyte fuel cell", *Journal of Electrochemical Society*, Vol. 139, No. 9, pp. 2477-2491, September 1992.

[7] J. Kim, S. Lee, and S. Srinivasan, "Modeling of proton exchange membrane fuel cell performance with an empirical equation", *Journal of Electrochemical Society*, Vol. 142, No. 8, pp. 2670-2674, August 1995.

[8] L. Song and J. W. Evans, "Electrochemical-thermal model of lithium polymer batteries", *Journal of Electrochemical Society*, Vol. 147, No. 6, pp. 2086-2095, 2000.

[9] J. Li, E. Murphy, J. Winnick and P. A. Kohl, "The effects of pulse charging on cycling characteristics of commercial lithium-ion batteries", *Journal of Power Sources*, Vol. 102, No. 1-2, pp.302-309, December 2001.

[10] T. Liu, D. Chen, and C. Fang, "Design and implementation of a battery charger with state-of-charge estimator", *International Journal of Electronics*, Vol. 87, No. 2, pp. 211-226, 2000.

[11] Z. Jiang, and R. Dougal, "Development of a fuel-cell-powered charging station for advanced technology batteries", to be published.

[12] T. Lovett, A Monti, E. Santi, R. Dougal, "A multilanguage environment for interactive simulation and development of controls for power electronics", *Proceedings of IEEE 32nd Annual Power Electronics Specialists Conference*, Vol. 3, pp. 1725 –1729, 2001.